AGU PUBLICATIONS

Geophysical Research Letters

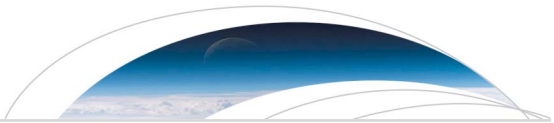

RESEARCH LETTER

10.1002/2015GL064081

Key Points:
- CryoSat-2 range measurements correlate with buoy-measured snow depth changes
- Assuming that CryoSat senses the ice freeboard is not justified for thick snow
- Arctic wide snow depth data are required

Supporting Information:
- Supporting Information S1
- Figure S1
- Figure S2

Correspondence to:
R. Ricker,
robert.ricker@awi.de

Citation:
Ricker, R., S. Hendricks, D. K. Perovich, V. Helm, and R. Gerdes (2015), Impact of snow accumulation on CryoSat-2 range retrievals over Arctic sea ice: An observational approach with buoy data, *Geophys. Res. Lett.*, *42*, doi:10.1002/2015GL064081.

Received 1 APR 2015
Accepted 16 MAY 2015
Accepted article online 21 MAY 2015

Impact of snow accumulation on CryoSat-2 range retrievals over Arctic sea ice: An observational approach with buoy data

Robert Ricker[1], Stefan Hendricks[1], Donald K. Perovich[2], Veit Helm[1], and Rüdiger Gerdes[1]

[1] Alfred Wegener Institute, Helmholtz Centre for Polar and Marine Research, Bremerhaven, Germany, [2] U.S. Army Cold Regions Research and Engineering Laboratory, Hanover, New Hampshire, USA

Abstract Radar altimetry measurements of the current satellite mission CryoSat-2 show an increase of Arctic sea ice thickness in autumn 2013, compared to previous years but also related to March 2013. Such an increase over the melting season seems unlikely and needs to be investigated. Recent studies show that the influence of the snow cover is not negligible and can highly affect the CryoSat-2 range retrievals if it is assumed that the main scattering horizon is given by the snow-ice interface. Our analysis of Arctic ice mass balance buoy records and coincident CryoSat-2 data between 2012 and 2014 adds observational evidence to these findings. Linear trends of snow and ice freeboard measurements from buoys and nearby CryoSat-2 freeboard retrievals are calculated during accumulation events. We find a positive correlation between buoy snow freeboard and CryoSat-2 freeboard estimates, revealing that early snow accumulation might have caused a bias in CryoSat-2 sea ice thickness in autumn 2013.

1. Introduction

A rapid reduction of the Arctic sea ice cover has been observed during the last decades [*Comiso et al.*, 2008; *Comiso*, 2012; *Comiso and Hall*, 2014; *Stroeve et al.*, 2012]. There is significant evidence that along with the shrinking ice area, sea ice is also thinning. This has been directly observed with upward looking sonar measurements from submarines, aircraft, and autonomous stations [*Rothrock et al.*, 1999; *Lindsay and Schweiger*, 2015; *Meier et al.*, 2014]. The only technique, however, to monitor sea ice thickness on basin scale are spaceborne satellite altimeter measurements [*Kwok et al.*, 2009; *Laxon et al.*, 2013]. The current satellite altimeter mission CryoSat-2 (CS-2) was launched in 2010 and is equipped with a K_u band synthetic aperture interferometric radar altimeter. CS-2 measures the ice surface and open water elevations. Subtracted, both quantities yield ice freeboard, the height of the ice above the local sea level. In contrast to a laser altimeter, such as on board the ice, cloud, and land elevation satellite (ICESat), the radar can penetrate the snow cover. The range estimate, and thus the freeboard sensed by the radar altimeter, depends on the actual location of the main scattering horizon [*Ricker et al.*, 2014] as well as surface roughness within the CS-2 footprint [*Hendricks et al.*, 2010]. In previous studies it has been assumed that the main scattering horizon is given by the snow-ice interface [*Laxon et al.*, 2013; *Kurtz et al.*, 2014], though both authors did not rule out an influence of radar backscatter from the snow layer. For K_u band frequencies (13.5 GHz), this assumption might only be valid for a cold, dry, and homogenous snow layer. On the other hand, density contrasts such as compacted snow and/or ice lenses in the snow layer may significantly alter the backscatter or absorption properties for K_u band signals [*Beaven et al.*, 1995]. *Kwok* [2014] analyzed airborne snow and K_u band radar data from Operation IceBridge and found that the air-snow interface clearly contributes to radar backscatter, causing an alteration of the tracking point. The limited CS-2 range resolution of 0.47 m does not allow to distinguish between the radar return of the snow-ice interface and the air-snow interface. Moreover, backscatter from both interfaces superimpose each other and cause broadened radar returns, which is largest for snow depths >20 cm [*Kwok*, 2014]. As a result, freeboard estimates can be biased high with the presence of thick snow layers. In addition, the effect of multiple backscatter interfaces on the radar waveform is superimposed by the effect of surface roughness in the CS-2 footprint. First retrieval methods obtain freeboard and roughness from CS-2 waveforms [*Kurtz et al.*, 2014]; however, the scale of snow contribution to the freeboard bias for different regions, ice types, and season is currently unclear. We therefore use the term radar freeboard, which is associated with CS-2 freeboard in this paper. It implies that surface roughness affects the range retrieval and that snow plays a role for the location of the main backscatter interface below the top snow surface. For wet snow at the

Table 1. Linear Trends α (cm/month) of Buoy Snow Freeboard (F_S), Buoy Ice Freeboard (F_I), and CryoSat-2 Modal Freeboard (F_C)[a]

Buoy	Event Period $[t_0, t_1]$	α_{F_S}	α_{F_I}	$\alpha_{F_{C40}}$	$\alpha_{F_{C50}}$	$\alpha_{F_{C80}}$
2012G-A	1 Oct 2012 to 30 Nov 2012	6.9 ± 0.6	-2.8 ± 0.3	1.8 ± 1.2	1.9 ± 1.2	1.6 ± 1.0
2012H	28 Sep 2012 to 29 Dec 2013	5.2 ± 0.4	-0.8 ± 0.1	4.8 ± 0.8	4.1 ± 0.7	3.3 ± 0.5
2012J	16 Oct 2012 to 13 Dec 2013	5.3 ± 0.7	-1.2 ± 0.4	4.9 ± 2.1	4.2 ± 1.7	3.2 ± 0.9
2012L	4 Apr 2012 to 18 May 2012	8.4 ± 0.6	-2.9 ± 0.3	$12.9^b \pm 3.4$	$9.3^b \pm 2.3$	$5.2^b \pm 1.5$
2012G-B	14 Sep 2013 to 9 Dec 2014	11.4 ± 1.0	-5.2 ± 0.4	8.3 ± 1.2	10.0 ± 2.0	6.5 ± 1.0
2013F	20 Sep 2013 to 1 Nov 2013	23.1 ± 1.1	-11.1 ± 0.6	12.5 ± 2.7	9.2 ± 1.9	4.8 ± 1.2
2013H	–	–	–	–	–	–

[a]For F_C different retracker thresholds have been applied: F_{C40} (40%), F_{C50} (50%), and F_{C80} (80%). The linear trends are calculated only during defined event periods (see Figure 3).
[b]No correction for lower wave propagation in the snow.

beginning and the end of the melting season, the dielectric properties of the snow layer might even limit the physical penetration of radar waves. It is our goal to estimate the uncertainties originating from additional snow backscatter and distinguish their effects from simplification or differences in waveform interpretations from available algorithms.

During the freeze up in November 2013, we observed increased multiyear ice freeboard compared to March 2013 of the CS-2 monthly gridded sea ice data product of the Alfred Wegener Institute [*Ricker et al.*, 2014]. An increase of freeboard over the melting season is not very likely and has to be investigated. However, few to none aircraft observations are available during this period. Ice mass balance buoys (IMBs), however, are deployed regularly in the Arctic and provide year-round measurements of sea ice thickness and snow depth. Their acoustic sounder measurements allow to monitor changes at the ice/snow surface and the ice bottom independently [*Richter-Menge et al.*, 2006]. Observational data from these buoys offer point measurements of ice thickness changes due to thermodynamic growth and the accumulation of snow. Furthermore, these data can be used to cross-validate satellite data [*Nghiem et al.*, 2007], although the comparison of spatial coarse satellite measurements with point measurements from IMBs can be problematic [*Kwok et al.*, 2007].

The importance of snow accumulation on freeboard retrieval during freeze up was investigated for the ICESat mission. Its laser altimeter is reflected at the top snow surface, and thus, the range measurements are a direct function of snow accumulation. Therefore, we use the term snow freeboard as the height of the snow surface above the water level. *Kwok et al.* [2007] compared ICESat snow freeboard measurements with values derived from IMB records in the Arctic and concluded that snow depth changes account for 90% of multiyear snow freeboard rise between autumn and late winter. Thus, any contribution of snow backscatter would cause a noticeable and temporal variable freeboard bias that is multiplied tenfold by the conversion into thickness.

In our study, we therefore compare IMB-derived sea ice thickness and snow depth with coincident CS-2 measurements between 2012 and 2014. This is done to investigate the observed increase of CS-2 multiyear sea ice freeboard north of Greenland and Canada over the melting season. We use the IMB data to investigate the changes of snow depth and CS-2 radar freeboard, avoiding the comparison between absolute values. We hypothesize that the snow cover significantly affects the CS-2 freeboard retrieval by snow backscatter which would affect also sea ice thickness and volume, independently of the range retrieval method.

2. Methods

2.1. Ice and Snow Freeboard From Ice Mass Balance Buoys

IMBs are usually deployed on undeformed sea ice floes of average size and thickness, avoiding deformed ice and melt ponds. The IMBs consist of a main buoy which carries the transmission and data acquisition system and batteries. Among other sensors, acoustic rangefinder sounders above the snow surface and below the ice bottom record changes in snow depth and bottom growth or ablation, respectively. The accuracy of these rangefinder sounders is 5 mm [*Richter-Menge et al.*, 2006].

We use provisional IMB data provided by *Perovich et al.* [2013] that are available on the website http://imb.erdc.dren.mil/buoysum.htm. They contain meteorological data and the positions of the snow surface, ice surface, and ice bottom. The range measurements are referenced to the initial ice surface. Hence, in the

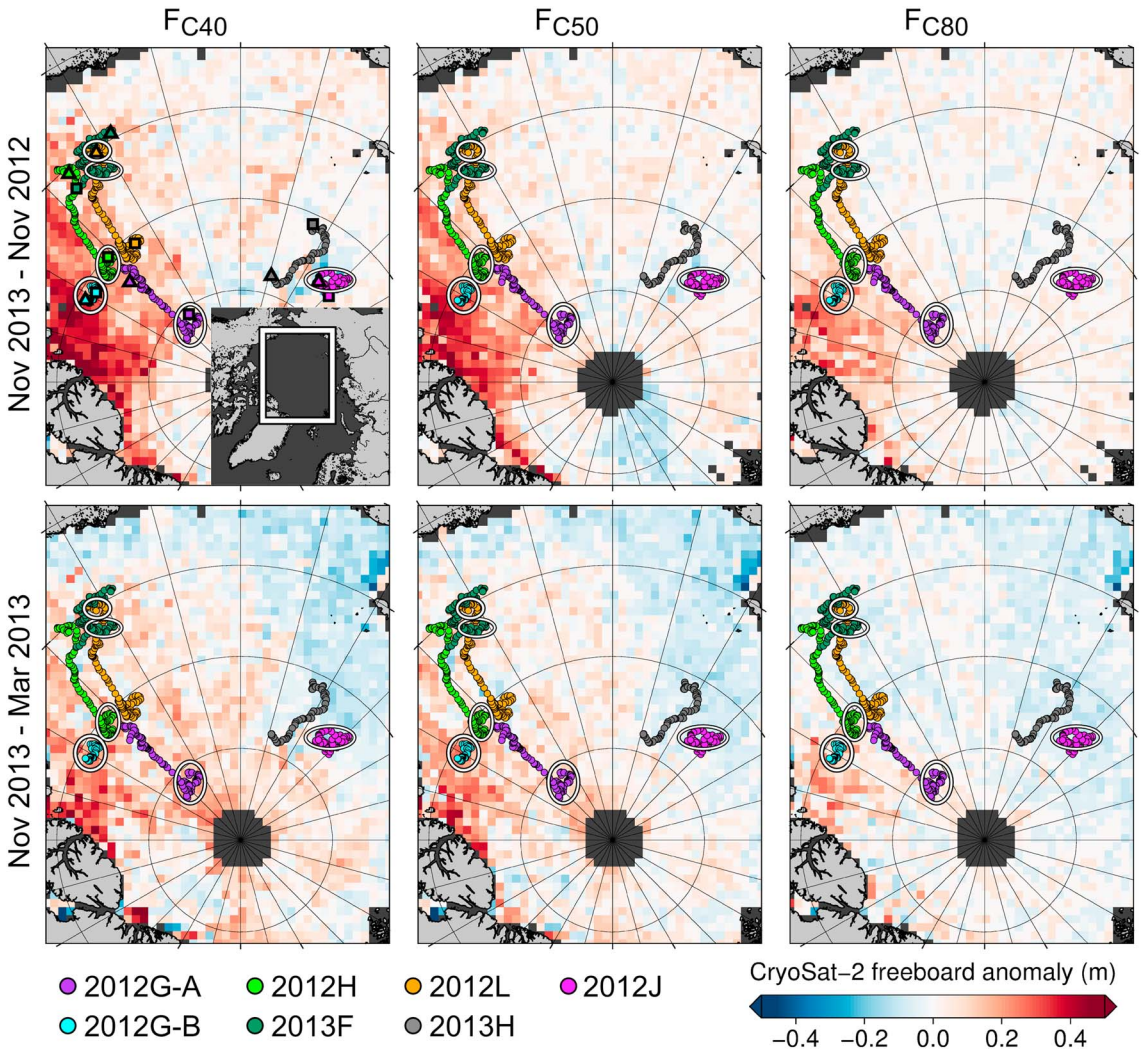

Figure 1. The maps show the differences in gridded CryoSat-2 Arctic modal freeboard (F_C) (top row) between November 2013 and November 2012 retrievals and (bottom row) between November 2013 and March 2013 retrievals. For F_C different retracker thresholds have been applied: F_{C40} (40%), F_{C50} (50%), and F_{C80} (80%). In addition, buoy tracks are mapped with encircled segments that represent the event periods where significant snow accumulation occurs (see Figure 3). Squares (triangles) in Figure 1(top left) highlight the start (end) of a considered buoy drift.

absence of ice surface melt the value of the ice bottom position is identical to the ice thickness. All consistent IMB data sets that were available in the period 2012–2014 are used in this study, in particular, the records of seven IMBs (Table 1). Figure 1 shows the IMB drift tracks within the considered period. The data set of IMB 2012G has been divided into two periods (A and B), since it covers two freezing seasons. We excluded data during summer season since CS-2 freeboard retrievals are not available for this period. Furthermore, periods where the rangefinder sensors became unreliable were excluded, except of IMB 2012G where the bottom sounder is unreliable from 7 September 2013 until 23 December 2013. We used a constant ice bottom position over the missing data period by using the last observed ice thickness of 2.16 m from 7 September 2013 onward. For an ice thickness of > 2 m and snow depth > 0.4 m the thermodynamic ice growth is < 0.1 m and therefore negligible [*Semtner*, 1976; *Leppäranta*, 1993].

The IMBs measure meteorological parameters hourly (position, barometric pressure, and air temperature) whereas others are sampled every 4 h (surface and bottom positions, temperature profiles). We resampled the IMB time series to a temporal resolution of 2 days, because with this period a sufficient CS-2 orbit coverage is given within a search radius of 50 km around an IMB position (Figure 2a). Since the IMB only measures

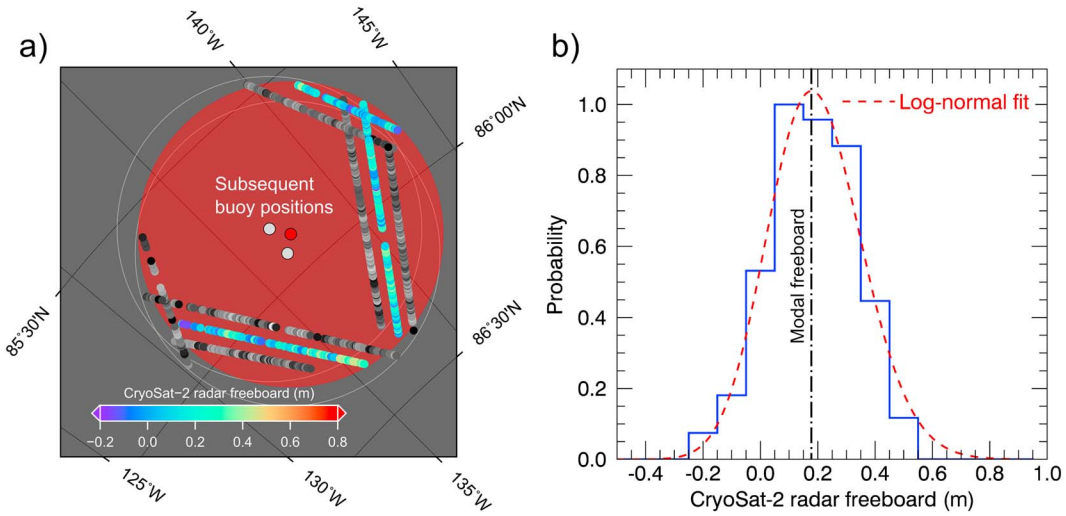

Figure 2. (a) Example of matched CryoSat-2 measurements within a 50 km radius (red circle) around a considered buoy position (red dot). Nearby, grey dots show the buoy position 2 days before and after the current position, together with the corresponding CryoSat-2 measurements (grey shaded). (b) Probability density function (blue solid line) of matched CryoSat-2 freeboard measurements for the considered buoy position in Figure 2a. The modal freeboard is retrieved by locating the maximum of the lognormal fit.

ice thickness (T) and snow depth (S), we have to convert them into ice (F_I) and snow freeboard (F_S), assuming hydrostatic equilibrium:

$$F_I = T \cdot \frac{\rho_W - \rho_I}{\rho_W} - S \cdot \frac{\rho_S}{\rho_W}, \quad (1)$$

$$F_S = F_I + S, \quad (2)$$

where densities of 320 [*Warren et al.*, 1999] and 1024 kg/m^3 are assumed for snow (ρ_S) and sea water (ρ_W). Since all considered IMBs were deployed at the end of the melting season or beginning of freeze up (see Table 1), we assume that the ice survived the summer melt and therefore used a multiyear ice density of 882.0 kg/m^3 [*Alexandrov et al.*, 2010]. We acknowledge that values for snow and multiyear ice densities vary in literature but since we consider relative changes, this effect should not be remarkable. We are also aware that the IMB spot measurements might not represent local hydrostatic equilibrium. We, however, assume that the observed snow accumulation is representative of nearby level ice.

2.2. CryoSat-2 Modal Freeboard Retrieval

CS-2 radar freeboard is obtained from ESA geolocated waveform data (Level-1B) and processed as described in *Ricker et al.* [2014]. We use the Threshold First-Maximum retracker [*Helm et al.*, 2014] with three different thresholds of 40%, 50%, and 80% [*Ricker et al.*, 2014] of the first-maximum peak power. This is done to investigate the influence of snow backscatter at different parts of the leading edge. We apply a range correction $h_c = h_a(1 - c_s/c_v)$ for a lower wave propagation speed inside the snow layer, where h_a is the apparent penetration, which is the covered distance in the snow when we assume vacuum speed of light (c_v) as propagation speed. It is estimated by the distance between the IMB snow freeboard and the respective CS-2 freeboard retrieval. The ratio of local speed of light in the snow layer (c_s) to c_v is approximately 0.78, assuming a snow density of 320 kg/m^3 [*Matzler and Wegmuller*, 1987; *Tiuri et al.*, 1984].

For the comparison with the IMB measurements, we apply a search radius of 50 km around each resampled IMB position within the given time window of 2 days. All individual CS-2 measurements within the search area are collected for further processing (Figure 2a). IMB measurement points are discarded if the number of matched CS-2 measurements is less than 50. The average number of matches is 206 for this analysis.

Since IMBs are usually deployed on level ice, we do not use the average of all collected CS-2 points. Instead, we compute the probability density functions of CS-2 freeboard values with a bin size of 10 cm and select

the modal value. To enhance the resolution and reduce noise, we compute a nonlinear least squares fit of a lognormal distribution of the CS-2 freeboard distribution:

$$f(x) = \frac{c}{\sigma(x-\vartheta)\sqrt{2\pi}} \cdot \exp\left(\frac{-(\ln(x-\vartheta)-\mu)^2}{2\sigma^2}\right). \quad (3)$$

Fit parameters are given by the logarithmical scale parameter (μ), the shape parameter (σ), the location parameter (ϑ), and a scale parameter for the lognormal distribution (c). The parameter x represents the thickness or bin value. The lognormal distribution describes typical sea ice thickness distributions [*Haas*, 2009]. Figure 2b shows an example of a CS-2 freeboard distribution and the corresponding fit within the search radius of a resampled IMB measuring point. We take the maximum of the lognormal fit to obtain the CS-2 modal freeboard at higher resolution than the binned values for comparison with the resampled IMB measurement.

3. Results

Figure 3 shows the direct comparison between the CS-2 modal freeboard retrievals and IMB snow and ice freeboard. We find high scattering of CS-2 modal freeboard, independent of the used retracker threshold. The sites where the IMBs were deployed show a high variability in ice thickness and snow depth. The observed mean thickness varies between values greater than 3 m (2012L) and less than 1 m (2012J). The thicker ice floes show no substantial growth during most parts of the freezing season (2012L), while snow accumulates mainly at the beginning of the freezing season between September and December. In order to find a correlation between snow depth and CS-2 freeboard, we focus on periods with substantial changes in snow depth that are marked in Figure 3 as event periods. We additionally restrict these periods by taking into account the left pulse peakiness (PP_L) that has been described in *Ricker et al.* [2014] and which is a measure of the width of the leading edge of the CS-2 waveforms. High values indicate a steep leading edge and a specular return while low values indicate a shallow leading edge. Specular returns typically originate from open or refrozen leads, or from melt ponds. As for the CS-2 freeboard (see section 2.2), we consider the modal PP_L. For example, along with IMB 2012J we find high modal PP_L values in September and October which gives evidence that open or refrozen melt ponds still dominate the ice surface and bias the CS-2 freeboard retrieval, since we consider waveforms that originate from sea ice only. We, therefore, exclude all periods from our analysis where the PP_L value exceeds 10.

We apply a linear regression model of the form f(t) = c + α t for measurements during the event periods (Figure 3) to find correlations between the individual data sets. The obtained linear trends α with 1 sigma uncertainties are presented in Table 1. IMB 2013H has been excluded because no significant change of the snow depth has been observed. For IMB 2012L the correction for lower wave propagation in snow has not been applied, since the CS-2 retrievals are consequently below the IMB ice freeboard and the approach according to section 2.2 is not reasonable. However, the impact of this correction on the trend is < 1 cm/month. We find only negative trends for the IMB ice freeboard, while IMB snow freeboard is always positive. The negative correlation between IMB snow and ice freeboard occurs due to the fact that an increasing snow load adds weight on the ice floe. On the other hand, we only find positive trends for the CS-2 modal freeboard. For example, along with IMB 2012G-B, we find rates of 8.3, 10.0, and 6.5 cm/month for the CS-2 modal freeboard retrievals by using 40%, 50%, and 80% retracker thresholds. For the same period we find a rate of 11.4 cm/month for the IMB snow freeboard and −5.2 cm/month for the IMB ice freeboard. This noticeable increase of the snow freeboard between September and December 2013 in conjunction with the simultaneous rise of the CS-2 modal freeboard is also shown in Figure 3.

The IMB drift tracks are mostly situated in regions where a positive CS-2 freeboard trend has been observed between March and November 2013 as well as between November 2012 and November 2013. The changes of CS-2 radar freeboard over the melting season in 2013 and between November 2012 and 2013 are shown as gridded freeboard difference maps for all retracker thresholds in Figure 1. The gridded differences are also based on modal freeboard, calculated in 5 cm bins, to be in line with the usage of modal freeboard in this study. We find high differences of up to 45 cm (30 cm) for the 40% threshold retrieval and up to 30 cm (20 cm) for the 80% threshold retrieval from the comparison between November 2013 and 2012 (November 2013 and March 2013) north of Canada.

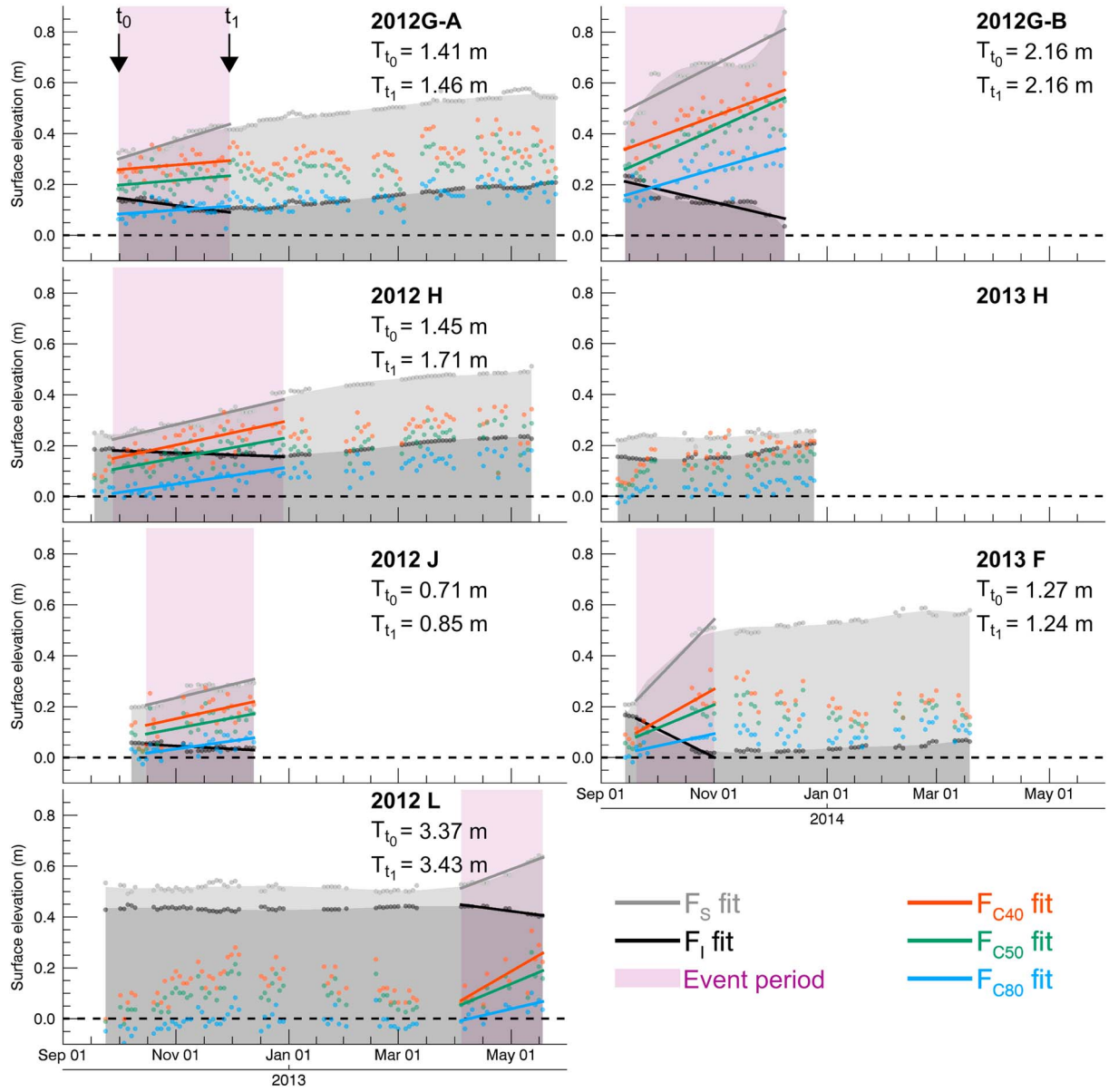

Figure 3. Time series of buoy snow freeboard (F_S), buoy ice freeboard (F_I), and CryoSat-2 modal freeboard (F_C). For F_C different retracker thresholds have been applied: F_{C40} (40%), F_{C50} (50%), and F_{C80} (80%). The solid lines represent the linear regression of freeboard from the individual measurements (dots). The purple boxes represent event periods, starting at t_0 and ending at t_1. During these periods, significant snow accumulation occurred and is considered for the linear regression (Table 1). T_{t_0} and T_{t_1} are the measured IMB ice thicknesses at t_0 and t_1.

4. Discussion

In all cases of snow accumulation during the event periods shown in Figure 3, the change of CS-2 radar freeboard was positive, while local observations at the IMB sites indicated decreasing ice freeboard in all cases (see also Figure S1 in the supporting information). The result is uniform for the three different retracker thresholds used in this study, which indicates a shift of the entire leading edge of the waveform. The comparison of absolute freeboard values reveals that the CS-2 retrieval using the highest threshold is closer to the IMB ice freeboard in typical cases, but there is no information of the statistical relevance of the IMB point data within its vicinity. In Figure 3 we find CS-2 freeboard retrievals located consequently below the ice freeboard of IMB 2012L for the entire considered period. This can have two reasons. Either the buoy is not in hydrostatic equilibrium or the multiyear ice (MYI) floe drifted in a regime of thinner first-year ice (see Figure 1). However, the

comparison between the absolute CS-2 and IMB freeboard retrievals can be problematic [*Kwok et al.*, 2007] and is not pursued in this study.

Nevertheless we expect that IMB-detected snowfall is representative of an area of 50 km around the buoy position, given that it is situated in the pack ice. In this case the findings indicate an increasing freeboard bias with snow accumulation and thus a higher bias for thick snow regimes, for example, multiyear ice zones. The prominent example for these regions is the IMB 2012G. Its observation period spans two freezing seasons, and in the second year, it remained in a confined area in the MYI region north of Canada (see Figure 1). During this time we also observe a substantial increase of CS-2 radar freeboard in the gridded product in November 2013, relative to November 2012, but also relative to March 2013 (see Figure 1). At the same time IMB 2012G shows thicker snow ($>$ 50 cm) in autumn 2013 than for 2012 ($\approx$ 30 cm). Whether the increase of CS-2 radar freeboard is an indication of earlier or heavier snowfall in 2013 or result of changing surface topography is unfortunately not known. In any case the radar freeboard in both years shows a correlation with the snow depth.

The observed average increase in CS-2 radar freeboard from March to November 2013 of about 18 cm north of Canada would imply a gain of at least 0.5 m in ice thickness if we assume typical values for MYI thickness (2 m) and snow depth (35 cm) in March and absence of snow cover in November as least extreme case. With the presence of snow also in November, the implied thickness gain would further increase if hydrostatic equilibrium is assumed. Thus, even a lower snow load in November cannot explain this substantial freeboard increase. Also, thermodynamic ice growth can be excluded, considering the absorbed and transmitted energy fluxes in Arctic summer [*Arndt and Nicolaus*, 2014].

Quick-look snow depth data, retrieved by Operation IceBridge (OIB) campaigns are provided by *Kurtz et al.* [2012, updated 2011] and show an increase of up to 20 cm between the freezing seasons 2012/2013 and 2013/2014 in spring north of Canada and in the Beaufort/Chukchi Sea (Figure S2). In contrast, other areas reveal a slight decrease. *Willatt et al.* [2010, 2011], *Kurtz et al.* [2014], *Kwok* [2014], and *Ricker et al.* [2014] showed that the influence of snow depth on the K_u band is not negligible. Specifically, the simulations of *Kwok* [2014] reveal that the snow-induced freeboard bias depends on the strength of snow surface backscatter and on the snow depth. The indication of an exceptional high snow depth in the freezing season 2013/2014 north of Canada by OIB strengthens the findings of our analysis. Our study, therefore, adds observational evidence to the findings of *Kwok* [2014]. Nevertheless, we also acknowledge that the OIB data are only provisional.

It is still difficult to quantify the snow-scatter-induced bias without knowledge of the regional distribution and temporal evolution of snow depth and snow stratigraphy. Snow, accumulated early, may undergo a partial melting and subsequent freezing as well as wind compaction. This leads to a very heterogeneous snow density distribution, while for the propagation of the K_u band signal it is widely assumed that the snow density is homogeneous. In this way, formed layers may affect the location of the main reflecting horizon. With snow accumulation starting already in September, when the CS-2 freeboard retrieval is still influenced by freezing or frozen melt ponds as indicated by the PP_L, we are not able to observe the beginning of this process. Likewise, wet snow or the start of snow melt in May defines the limit of retrievable CS-2 freeboard data. A model-based investigation of K_u band radar backscatter for observed snow condition that includes internal layering and a range of metamorphic states would be helpful as a step toward the quantification of a snow bias on CS-2 data. With the differences between trends α_{F_C} and α_{F_I}, given in Table 1, we can estimate the freeboard-induced impact T_{bias} on the CS-2 thickness retrieval within the event periods:

$$T_{\text{bias}} = \frac{\partial T}{\partial F} \int_{t_0}^{t_1} (\alpha_{F_C} - \alpha_{F_I})\, \mathrm{d}t = \left(\frac{\rho_W}{\rho_W - \rho_I} \right) (\alpha_{F_C} - \alpha_{F_I})(t_1 - t_0), \tag{4}$$

where $\frac{\partial T}{\partial F}$ represents CS-2 sea ice thickness (T), derived from equation (2) and differentiated with respect to freeboard (F). The parameters t_0 and t_1 mark the start and end of the event period, respectively (see Figure 3). Averaged over all three threshold retrievals, we obtain biases T_{bias} between 0.7 m (2012G-A) and 2.7 m (2012G-B) while the mean thickness bias is 1.4 m. Thus, our findings suggest significant thickness biases over multiyear ice with thick snow layers, if it is generally assumed that the main scattering horizon is given by the snow-ice interface during freeze up.

The CS-2 freeboard retrievals feature random and systematic uncertainties. Speckle noise is the major contribution to the random uncertainties. For the gridded product (Figure 1), they are below 5 cm while for a single buoy-referenced modal freeboard retrieval (Figure 3), the uncertainty is in the range of 10 cm (one

bin, respectively). Any systematic uncertainties are expected to have a correlation length higher than the respective search area (50 km radius) and thus should not have a significant impact on the linear trends in Table 1. The sea surface height uncertainty can be either random or systematic, depending on the interpolation between leads. In any case this uncertainty is represented by the scatter of the CS-2 modal freeboard values (see Figure 3) and in the 1 sigma uncertainties of the trends.

The random uncertainties of the IMB measurements are attributed to their accuracy of 5 mm and hence are negligible in this comparison. Potential biases can occur due to the thickness to freeboard conversion where we use constant values for ice and snow densities. However, relative changes and trends should not be affected remarkably. Another origin of uncertainty is snow drift that occurs on site and counteracts the larger scale correlation of the IMB snow depth measurements. This impact should be reduced by considering measurements of seven independently operating IMBs.

5. Conclusion

We hypothesized that the CryoSat-2 freeboard retrieval is affected by snow accumulation, causing a bias that has contributed to the major increase of CryoSat-2 multiyear ice freeboard north of Canada in November 2013. We compared year-round ice and snow freeboard measurements of Arctic ice mass balance buoys (IMBs) from 2012 to 2014 with coincident CryoSat-2 measurements. We used CryoSat-2 modal freeboard retrievals by applying three different retracker thresholds to investigate the effect of snow accumulation on different parts of the leading edge.

By defining event periods of substantial snow depth changes, we calculated linear trends of the CryoSat-2 freeboard retrievals and IMB ice and snow freeboard within these periods. We only find negative trends for the IMB ice freeboard while the IMB snow freeboard trends are always positive. Simultaneously, we observe only positive trends for coincident CryoSat-2 radar freeboard estimates, regardless of the used retracker threshold. North of Canada we find a mean increase of 18 cm of the gridded CryoSat-2 freeboard retrieval from March to November 2013. From September to December 2013 IMB measurements in this area reveal snow and ice freeboard growth rates of 11.4 and −5.2 cm/month, respectively. At the same time we find a mean CryoSat-2 freeboard growth rate of 8.3 cm/month, averaged over all three retracker retrievals. We do assume that this observation is the result of a snow bias on CryoSat-2 freeboard data, since thermodynamic ice growth over the summer period is not to be expected. The magnitude of this bias is larger than reported values in literature that were based on theoretical considerations [*Kurtz et al.*, 2014; *Kwok*, 2014]. An exceptional high snow depth and early accumulation during the freezing season 2013/2014 north of Canada, shown by IMB measurements and indicated by Operation IceBridge snow depth retrievals, might have lead to the major increase of CryoSat-2 multiyear ice freeboard in November 2013 for this region. By quantifying the impact on CryoSat-2 sea ice thickness retrievals, we obtain a mean multiyear ice thickness bias of 1.4 m, if it is assumed that the main scattering horizon is given by the snow-ice interface.

We conclude that snowfall can have a significant impact on CryoSat-2 range measurements and therefore on ice freeboard, thickness, and volume. The assumption that the CryoSat-2 main scattering horizon is given by the snow-ice interface cannot be justified in regions with a thick snow layer. Finally, this study also shows that there is a strong need for more data and knowledge about the seasonal cycle of snow distribution and properties on sea ice.

Acknowledgments
Ice mass balance buoy data are provided by the Cold Regions Research and Engineering Laboratory (CRREL). CryoSat-2 data are provided by the European Space Agency (ESA). The work of S. Hendricks and V. Helm was funded by the German Federal Ministry of Economics and Technology (grant 50EE1008). All this is gratefully acknowledged. Thanks also to Marcel Nicolaus and Sandra Schwegmann for their input.

The Editor thanks two anonymous reviewers for their assistance in evaluating this paper.

References

Alexandrov, V., S. Sandven, J. Wahlin, and O. M. Johannessen (2010), The relation between sea ice thickness and freeboard in the Arctic, *Cryosphere*, *4*(3), 373–380, doi:10.5194/tc-4-373-2010.

Arndt, S., and M. Nicolaus (2014), Seasonal cycle and long-term trend of solar energy fluxes through Arctic sea ice, *Cryosphere*, *8*(6), 2219–2233, doi:10.5194/tc-8-2219-2014.

Beaven, S. G., G. L. Lockhart, S. P. Gogineni, A. R. Hossetnmostafa, K. Jezek, A. J. Gow, D. K. Perovich, A. K. Fung, and S. Tjuatja (1995), Laboratory measurements of radar backscatter from bare and snow-covered saline ice sheets, *Int. J. Remote Sens.*, *16*(5), 851–876, doi:10.1080/01431169508954448.

Comiso, J. C. (2012), Large decadal decline of the arctic multiyear ice cover, *J. Clim.*, *25*(4), 1176–1193.

Comiso, J. C., and D. K. Hall (2014), Climate trends in the Arctic as observed from space, *Wiley Interdiscip. Rev. Clim. Change*, *5*(3), 389–409.

Comiso, J. C., C. L. Parkinson, R. Gersten, and L. Stock (2008), Accelerated decline in the Arctic sea ice cover, *Geophys. Res. Lett.*, *35*, L01703, doi:10.1029/2007GL031972.

Haas, C. (2009), Dynamics versus thermodynamics: The sea ice thickness distribution, in *Sea Ice*, vol. 2, edited by D. N. Thomas and G. S. Diekmann, chap. 4, pp. 113–151, Wiley-Blackwell, Oxford, U. K.

Helm, V., A. Humbert, and H. Miller (2014), Elevation and elevation change of Greenland and Antarctica derived from CryoSat-2, *Cryosphere*, *8*(4), 1539–1559, doi:10.5194/tc-8-1539-2014.

Hendricks, S., L. Stenseng, V. Helm, and C. Haas (2010), Effects of surface roughness on sea ice freeboard retrieval with an airborne Ku-band SAR radar altimeter, paper presented at IEEE International Geoscience and Remote Sensing Symposium, IGARSS, pp. 25–30, July 2010.

Kurtz, N., M. S. Studinger, J. Harbeck, V. Onana, and S. Farrell (2012, updated 2014), *IceBridge Sea Ice Freeboard, Snow Depth, and Thickness*, NASA National Snow and Ice Data Center Distributed Active Archive Center, Boulder, Colo. [Available at http://dx.doi.org/10.5067/7XJ9HRV50O57.]

Kurtz, N. T., N. Galin, and M. Studinger (2014), An improved CryoSat-2 sea ice freeboard retrieval algorithm through the use of waveform fitting, *Cryosphere*, *8*(4), 1217–1237, doi:10.5194/tc-8-1217-2014.

Kwok, R. (2014), Simulated effects of a snow layer on retrieval of CryoSat-2 sea ice freeboard, *Geophys. Res. Lett.*, *41*, 5014–5020, doi:10.1002/2014GL060993.

Kwok, R., G. F. Cunningham, H. J. Zwally, and D. Yi (2007), Ice, cloud, and land elevation satellite (ICESat) over Arctic sea ice: Retrieval of freeboard, *J. Geophys. Res.*, *112*, C12013, doi:10.1029/2006JC003978.

Kwok, R., G. F. Cunningham, M. Wensnahan, I. Rigor, H. J. Zwally, and D. Yi (2009), Thinning and volume loss of the Arctic Ocean sea ice cover: 2003–2008, *J. Geophys. Res.*, *114*, C07005, doi:10.1029/2009JC005312.

Laxon, S. W., et al. (2013), CryoSat-2 estimates of Arctic sea ice thickness and volume, *Geophys. Res. Lett.*, *40*, 732–737, doi:10.1002/grl.50193.

Leppäranta, M. (1993), A review of analytical models of sea-ice growth, *Atmos. Ocean*, *31*(1), 123–138.

Lindsay, R., and A. Schweiger (2015), Arctic sea ice thickness loss determined using subsurface, aircraft, and satellite observations, *Cryosphere*, *9*(1), 269–283, doi:10.5194/tc-9-269-2015.

Matzler, C., and U. Wegmuller (1987), Dielectric properties of freshwater ice at microwave frequencies, *J. Phys. D*, *20*, 1623–1630, doi:10.1088/0022-3727/20/12/013.

Meier, W. N., et al. (2014), Arctic sea ice in transformation: A review of recent observed changes and impacts on biology and human activity, *Rev. Geophys.*, *52*, 185–217, doi:10.1002/2013RG000431.

Nghiem, S. V., I. G. Rigor, D. K. Perovich, P. Clemente-Colón, J. W. Weatherly, and G. Neumann (2007), Rapid reduction of Arctic perennial sea ice, *Geophys. Res. Lett.*, *34*, L19504, doi:10.1029/2007GL031138.

Perovich, D., J. Richter-Menge, B. Elder, T. Arbetter, K. Claffey, and C. Polashenski (2013), Observing and understanding climate change: Monitoring the mass balance, motion, and thickness of Arctic sea. [Available at http://IMB.crrel.usace.army.mil.]

Richter-Menge, J. A., D. K. Perovich, B. C. Elder, K. Claffey, I. Rigor, and M. Ortmeyer (2006), Ice mass-balance buoys: A tool for measuring and attributing changes in the thickness of the Arctic sea-ice cover, *Ann. Glaciol.*, *44*(1), 205–210.

Ricker, R., S. Hendricks, V. Helm, H. Skourup, and M. Davidson (2014), Sensitivity of CryoSat-2 Arctic sea-ice freeboard and thickness on radar-waveform interpretation, *Cryosphere*, *8*(4), 1607–1622, doi:10.5194/tc-8-1607-2014.

Rothrock, D. A., Y. Yu, and G. A. Maykut (1999), Thinning of the Arctic sea-ice cover, *Geophys. Res. Lett.*, *26*(23), 3469–3472, doi:10.1029/1999GL010863.

Semtner, A. J., Jr. (1976), A model for the thermodynamic growth of sea ice in numerical investigations of climate, *J. Phys. Oceanogr.*, *6*(3), 379–389.

Stroeve, J., M. Serreze, M. Holland, J. Kay, J. Malanik, and A. Barrett (2012), The Arctic's rapidly shrinking sea ice cover: A research synthesis, *Clim. Change*, *110*(3–4), 1005–1027, doi:10.1007/s10584-011-0101-1.

Tiuri, M. E., A. Sihvola, E. Nyfors, and M. Hallikaiken (1984), The complex dielectric constant of snow at microwave frequencies, *IEEE J. Oceanic Eng.*, *9*(5), 377–382, doi:10.1109/JOE.1984.1145645.

Warren, S. G., I. G. Rigor, N. Untersteiner, V. F. Radionov, N. N. Bryazgin, Y. I. Aleksandrov, and R. Colony (1999), Snow depth on Arctic sea ice, *J. Clim.*, *12*(6), 1814–1829.

Willatt, R., K. Giles, S. Laxon, L. Stone-Drake, and A. Worby (2010), Field investigations of Ku-band radar penetration into snow cover on Antarctic sea ice, *IEEE Trans. Geosci. Remote Sens.*, *48*(1), 365–372, doi:10.1109/TGRS.2009.2028237.

Willatt, R., S. Laxon, K. Giles, R. Cullen, C. Haas, and V. Helm (2011), Ku-band radar penetration into snow cover on Arctic sea ice using airborne data, *Ann. Glaciol.*, *52*(57), 197–205.